Mat. Res. Soc. Symp. Proc. Vol. 789 © 2004 Materials Research Society N16.9.1

Probing the Long Range Distance Dependence of Noble Metal Nanoparticles

Amanda J. Haes and Richard P. Van Duyne
Northwestern University, Department of Chemistry, 2145 Sheridan Road
Evanston, Illinois 60208-3113, U.S.A.

ABSTRACT

The localized surface plasmon resonance (LSPR) of noble metal nanoparticles has recently been the subject of extensive studies. Previously, it has been demonstrated that Ag nanotriangles that have been synthesized using nanosphere lithography (NSL) behave as extremely sensitive and selective chemical and biological sensors. The present work reveals information regarding the long range distance dependence of the localized surface plasmon resonance (LSPR) of silver and gold nanoparticles. Multilayer adsorbates based on the interaction of $HOOC(CH_2)_{10}SH$ and Cu^{2+} were assembled onto surface-confined nanoparticles. Measurement of the LSPR extinction peak shift versus number of layers and adsorbate thickness is non-linear and has a sensing range that is dependent on the composition, shape, in-plane width, and out-of-plane height of the nanoparticles. Theoretical modeling confirms and offers a mathematical interpretation of these results. These experiments indicate that the LSPR sensing capabilities of noble metal nanoparticles can be tuned to match the size of biological and chemical analytes by adjusting the aforementioned properties. The optimization of the LSPR nanosensor for a specific analyte will improve an already sensitive nanoparticle-based sensor.

INTRODUCTION

For ~20 years, surface plasmon resonance (SPR) sensors, that is, copper, gold, or silver planar films have been used as refractive index based sensing devices to detect analyte binding at or near a metal surface.[1] This sensor exhibits an extremely large refractive index sensitivity (~$2x10^6$ nm/RIU) and modest decay length (200-300 nm),[2] and this sensitivity is proportional to the square of the electric field that extends from the metal film. Recently, it was realized that this refractive index sensitivity also exists for noble metal nanoparticles. Although it has been demonstrated to operate successfully for nanoparticles, details regarding the aforementioned properties of planar SPR sensors still need a more complete explanation.

Advancements in technology due to nanoscale phenomena of materials will be made and/or optimized when the chemical and physical properties of materials are more thoroughly understood. Prior to the realization of this technology, methods to synthesize isolated monodisperse nanoparticles in a controlled environment must be developed and their properties must be thoroughly characterized.

The development of nanoparticle-based optical sensors is an extremely active area of nanoscience research. One such nanoparticle based optical sensor is known as the localized surface plasmon resonance (LSPR) nanosensor. The LSPR of noble metal nanoparticles arises when electromagnetic radiation induces a collective oscillation of the conduction electrons of the individual nanoparticles and has two primary consequences: (1) selective photon absorption which allows the optical properties of these nanoparticles to be monitored with UV-visible spectroscopy and (2) the enhancement of the electromagnetic fields surrounding the nanoparticles which is responsible for all surface-enhanced spectroscopies.

Recently, we found that a result of this phenomenon is the extreme sensitivity of nanoparticles to changes in its surrounding dielectric environment. For this reason, we have developed a sensing scheme based on this property. In order to understand and optimize this sensing platform, the goal of this work is to achieve a better comprehension of the electromagnetic fields surrounding the nanoparticle. Specifically, the elucidation of the long range distance dependence of the LSPR of surface confined noble metal nanoparticles will assist in the optimization of the LSPR nanosensor.

EXPERIMENTAL DETAILS

Materials

11-Mercaptoundecanoic acid (11-MUA) and $Cu(ClO_4)_2$ were purchased from Aldrich (Milwaukee, WI). Absolute ethanol was purchased from Pharmco (Brookfield, CT). Hexanes and methanol were purchased from Fisher Scientific (Pittsburgh, PA). Ag wire (99.99%, 0.5 mm diameter) and Au wire (99.9%, 0.025 mm diameter) was obtained from D. F. Goldsmith (Evanston, IL). Borosilicate glass substrates, No. 2 Fisherbrand 18 mm circle coverslips were purchased from Fisher Scientific (Pittsburgh, PA). Tungsten vapor deposition boats were acquired from R. D. Mathis (Long Beach, CA). Polystyrene nanospheres with diameters of 280±4 nm, 310±9 nm, 400±8 nm, 450±5 nm, and 510±11 nm were received as a suspension in water (Interfacial Dynamics Corporation, Portland, OR) and were used without further treatment. Millipore cartridges (Marlborough, MA) were used to purify water to a resistivity of 18 $M\Omega cm^{-1}$. All materials were used without further purification.

Substrate Preparation

Glass substrates were cleaned in a piranha solution (1:3 30 % H_2O_2:H_2SO_4) at 80°C for 30 minutes. Once cooled, the glass substrates were rinsed with copious amounts of water and then sonicated for 60 minutes in 5:1:1 H_2O:NH_4OH:30% H_2O_2. Next, the glass was rinsed repeatedly with water and was stored in water until used.

Nanoparticle Preparation

NSL was used to fabricate monodisperse, surface-confined Ag nanoparticles (Figure 1).[3, 4] For these experiments, single layer colloidal crystal nanosphere masks were prepared by drop coating ~2 μL of nanosphere solution onto glass substrates. Once the nanosphere masks were dry, the substrates were mounted into a Consolidated Vacuum Corporation vapor deposition system. A Leybold Inficon XTM/2 quartz crystal microbalance (East Syracuse, NY) was used to measure the thickness of the Ag or Au film deposited over the nanosphere mask, d_m. Following metal deposition, the nanosphere mask was removed by sonicating the sample in ethanol for 3 minutes. The perpendicular bisector of the nanoparticles, a, was varied by changing the diameter, D, of the nanospheres used. The samples were either thermally annealed for 1 hour at ~600°C in the aforementioned chamber or solvent annealed. Unless otherwise noted, all samples were stabilized by solvent annealing. While the solvent slightly restructures the nanoparticles, that is, causes slight rounding of the nanotriangle tips, the overall triangular footprint is retained, and in this process, also produces stable extinction maxima readings in a

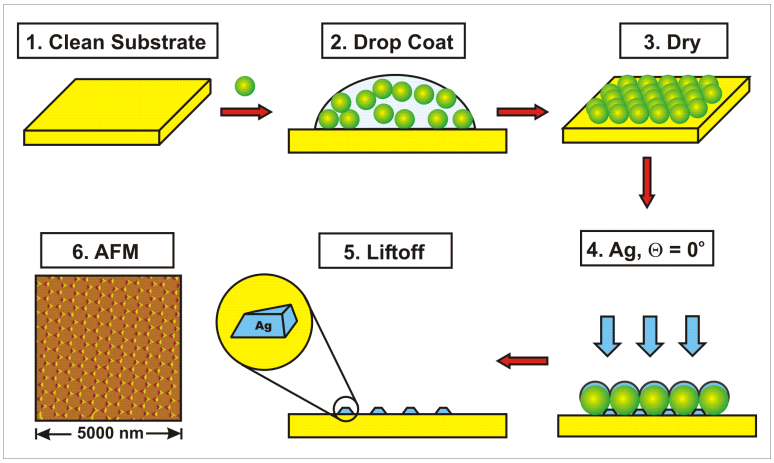

Figure 1. Ag nanoparticles were fabricated using NSL. Six steps are required for the synthesis of the nanoparticles: (1) glass or mica substrates are cleaned, (2) monodisperse polystyrene nanospheres are drop-coated onto the substrate, (3) a single layer of hexagonally close packed nanospheres dries creating a nanosphere mask, (4) Ag metal is vapor deposited onto the sample, (5) the nanosphere mask is removed via sonication in ethanol, and (6) the Ag nanoparticle sample is prepared for sensing experiments.

given environment. Thermal annealing is performed to convert the nanotriangles into nanohemispheres. A comparison between the two annealing methods enables the study of LSPR sensing as a function of nanoparticle shape.

Ultraviolet-visible Extinction Spectroscopy

Macroscale UV-vis extinction measurements were collected using an Ocean Optics (Dunedin, FL) SD2000 fiber optically coupled spectrometer with a CCD detector. All spectra collected are macroscopic measurements performed in standard transmission geometry with unpolarized light. The probe beam diameter was approximately 2 mm.

Nanoparticle Annealing

A home built flow cell[5] was used to control the external environment of the Ag nanoparticle substrates. Prior to modification, the Ag nanoparticles were solvent annealed.[5] Dry N_2 gas and solvent were cycled through the flow cell until the λ_{max} of the sample stabilized.

Nanoparticle Functionalization

After solvent annealing, the nanoparticle samples were functionalized with 1 mM 11-MUA (ethanol) solutions. Within 10 minutes, the extinction maximum of the sample stabilized and the sample was rinsed with copious amounts of ethanol. At this point, the sulfhydryl group binds to the Ag surface, thus placing the carboxylic acid group away from the surface. Next, a 1 mM $Cu(ClO_4)_2$ (ethanol) was exposed to the sample until the extinction maximum peak had stabilized (less than 3 minutes). The sample cell was flushed with ethanol, and the extinction spectrum of the sample in N_2 was collected. The Cu^{2+} ions interact with the surface-confined carboxylic acid

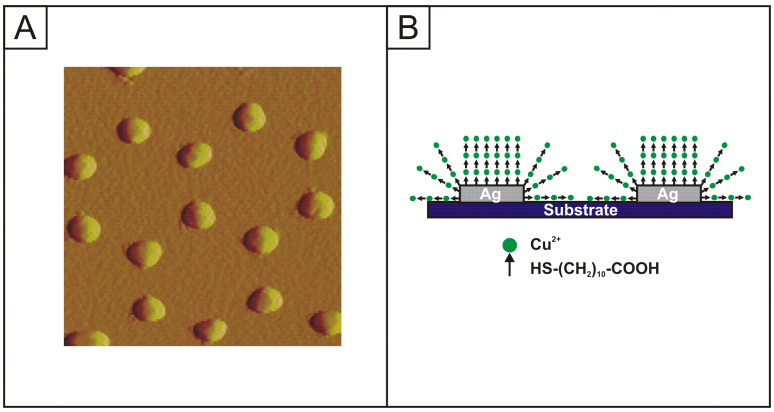

Figure 2. (A) AFM image of thermally annealed Ag nanoparticles. Ag nanoparticles were first synthesized using NSL. Following that process, the samples were then placed in a high vacuum chamber and heated to induced nanoparticle annealing. The resulting nanoparticle have in-plane widths of 110 nm and out-of-plane heights of 61 nm. The image is 1 μm x 1 μm. (B) Binding chemistry of the multilayer SAMs. One layer consists of 11-mercaptoundecanoic acid and Cu^{2+}.

groups. This represents one layer. A new layer is initiated by the introduction of 11-MUA. The sulfhydryl groups interact with the surface-confined Cu^{2+} ions, etc. These functionalization steps were repeated until the extinction maximum no longer shifted.

Atomic Force Microscopy (AFM)

AFM images were collected using a Digital Instruments Nanoscope IV microscope and Nanoscope IIIa controller operating in tapping mode. Etched Si nanoprobe tips (TESP, Digital Instruments, Santa Barbara, CA) were used. These tips had resonance frequencies between 280 and 320 kHz and are conical in shape with a cone angle of 20° and an effective radius of curvature at the tip of 10 nm. The image shown in Figure 2A that represents a thermally annealed sample is unfiltered data that were collected in ambient conditions. The height of the nanoparticles, b, was determined using AFM.

RESULTS AND DISCUSSION

The metal ion, carboxylated alkanethiol self-assembled monolayer (SAM) has many desirable characteristics (Figure 2B):[6, 7] (1) the first alkanethiol layer forms with the thiol group on the metal surface with no significant mixing of molecule orientation, (2) the second (and additional) alkanethiol layer forms with the same orientation as the first, (3) the first two alkanethiol layers have approximately equal number of molecules, (4) 20+ uniform layers can be formed, and (5) the refractive index of the layer is constant and assumed to be ~1.5 to 1.6 depending on layer ordering.[6 8] The exact binding of the alkanethiol to the metal ions is unclear. X-ray photoelectron spectroscopy studies indicate that 1 to 8 metal ions coordinate to every 2 carboxyl groups. Despite this unknown interaction, this multilayer structure offers a simple, controlled way to probe the long range distance dependence, and correspondingly, the electromagnetic field strength 10+ nm away from the nanostructured surfaces.[9]

Shape Influences on LSPR Long Range Dependence

The UV-vis extinction spectra for thermally annealed Ag nanoparticles (a = 110 nm, b = 61 nm) with 0 - 20 SAM layers is found in Figure 3A. Several distinctive features can be discerned from this data. As the adsorbate layer thickness increases, the extinction maximum red shifts, the full width half maximum (FWHM) remains approximately constant (100±10 nm), and the peak intensity increases. At layer 16, the extinction maximum stops shifting, the FWHM begins increasing, and the peak intensity begins to decrease. These three diagnostic features signal that of the sensing volume of the nanoparticle had been saturated.

An example of the LSPR extinction maximum shift from bare nanotriangles and nanohemispheres versus multilayer thickness (as determined by AFM) is displayed in Figures 3B. In this study, nanotriangles were synthesized on a glass substrate using nanospheres (D = 400 nm) and 50.0 nm of Ag metal. After nanosphere removal (in the case of Figure 3B), the samples were placed in a high vacuum chamber where they were thermally annealed for 1 hour at ~600°C. The nanotriangles (a = 114 nm, b = 54 nm) were converted into nanohemispheres (a = 110 nm, b = 61 nm) during this process. In both cases, the samples were stabilized in solvent and exposed to the appropriate molecular solution. In all cases, incubation in 11-MUA and $Cu(ClO_4)_2$ constitutes one layer. It is evident that even at low multilayer thicknesses, the nanotriangles give larger LSPR responses than the nanohemispheres. This result is consistent with studies done on identically prepared samples where the LSPR shift induced from hexadecanethiol was larger for nanotriangles than for nanohemispheres.[10] Additionally, theoretical studies support that as nanoparticles become more spherical, the electromagnetic field strength at their surface decreases.[11, 12] This indicates that the electromagnetic fields at the nanoparticle surface are more intense for nonhemispherical nanoparticles. Finally, because

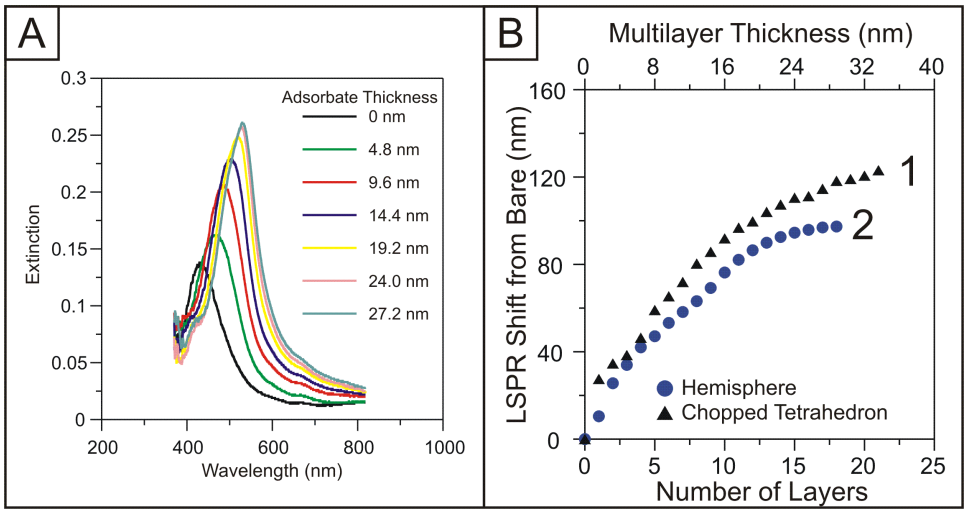

Figure 3. (A) Long range LSPR spectroscopy of Ag nanoparticles (a = 110 nm, b = 61.0 nm) for 0 - 17 layers of Cu^{2+}/$HS\text{-}CH_2)_{10}COOH$. All extinction measurements were collected in a N_2 environment. (B) Shape dependence on the long range LSPR distance dependence for Ag nanoparticles (D = 400 nm). (B-1) LSPR shift vs. Number of SAM layers/layer thickness for solvent annealed Ag nanoparticles. (B-2) LSPR shift vs. Number of SAM layers/layer thickness for thermally annealed (600°C for 1 hour) Ag nanoparticles.

nanotriangles exhibit larger total LSPR shifts and can detect molecules larger distances away from the nanoparticle surface, their electromagnetic fields strength and sensing volumes are both larger.

CONCLUSION

It was suspected that the linear distance dependence found in our previous alkanethiol self-assembled monolayer (SAM) formation studies was the thin shell limit of a longer range, nonlinear dependence. To verify this, a multilayer SAM shell approach based on the interaction of $HOOC(CH_2)_{10}SH$ and Cu^{2+} was used and were allowed to assemble onto surface-confined noble metal nanoparticles, and monitored their properties using UV-visible spectroscopy. Measurement of the LSPR extinction peak shift versus number of layers and adsorbate thickness is non-linear and has a sensing range that is dependent on the composition,[13] shape,[13] in-plane width,[13] and out-of-plane height[13] of the nanoparticles. Specifically, the following long range aspects of the LSPR nanosensor was demonstrated: (1) the LSPR shift versus number of adsorbate layers and adsorbate thickness is non-linear and (2) nanotriangles have larger sensing volumes and are more sensitive to multilayer adsorbates than nanohemispheres of equal volume. This optimization when coupled with additional size and composition studies and theoretical studies[13] is allowing us to significantly improve an already sensitive nanoparticle-based sensor.

ACKNOWLEDGEMENTS

The authors gratefully acknowledge support from the Nanoscale Science and Engineering Initiative of the National Science Foundation under NSF Award Number EEC-0118025. Any opinions, findings and conclusions or recommendations expressed in this material are those of the authors and do not necessarily reflect those of the National Science Foundation. A. Haes also wishes to acknowledge the American Chemical Society Division of Analytical Chemistry and Dupont for fellowship support.

REFERENCES

1. J. M. Brockman, B. P. Nelson and R. M. Corn, Annu. Rev. Phys. Chem. **51**, 41 (2000).
2. L. S. Jung, C. T. Campbell, T. M. Chinowsky, M. N. Mar and S. S. Yee, Langmuir **14**, 5636 (1998).
3. J. C. Hulteen and R. P. Van Duyne, J. Vac. Sci. Technol. A **13**, 1553 (1995).
4. C. L. Haynes and R. P. Van Duyne, J. Phys. Chem. B **105**, 5599 (2001).
5. M. D. Malinsky, K. L. Kelly, G. C. Schatz and R. P. Van Duyne, J. Am. Chem. Soc. **123**, 1471 (2001).
6. S. D. Evans, T. M. Flynn and A. Ulman, Langmuir **11**, 3811 (1995).
7. T. L. Freeman, S. D. Evans and A. Ulman, Langmuir **11**, 4411 (1995).
8. S. D. Evans, Personal Communication (2003).
9. A. Hatzor and P. S. Weiss, Science **291**, 1019 (2001).
10. A. J. Haes and R. P. Van Duyne, J. Am. Chem. Soc. **124**, 10596 (2002).
11. E. J. Zeman and G. C. Schatz, J. Phys. Chem. **91**, 634 (1987).
12. T. R. Jensen, K. L. Kelly, A. Lazarides and G. C. Schatz, J. Cluster Sci. **10**, 295 (1999).
13. A. J. Haes, S. Zou, G. C. Schatz and R. P. Van Duyne, J. Phys. Chem. B In Press (2003).